

ZnO metal–semiconductor–metal ultraviolet photodetectors with Iridium contact electrodes

S.J. Young, L.W. Ji, S.J. Chang, Y.P. Chen, K.T. Lam, S.H. Liang, X.L. Du, Q.K. Xue and Y.S. Sun

Abstract: ZnO epitaxial films were grown on sapphire (0001) substrates by using rf plasma-assisted molecular beam epitaxy. Metal–semiconductor–metal (MSM) photodetectors with Iridium (Ir) electrodes were then fabricated. It was found that Schottky barrier heights at the non-annealed and 500°C-annealed Ir/ZnO interfaces were around 0.65 and 0.78 eV, respectively. With an incident wavelength of 370 nm and 1 V applied bias, it was found that the maximum responsivities for the Ir/ZnO/Ir MSM photodetectors with and without thermal annealing were 0.18 and 0.13 A/W, respectively. From transient response measurement, it was found that time constant τ of the fabricated photodetectors was 22 ms. For a given bandwidth of 100 Hz and 1 V applied bias, we found that noise equivalent power and corresponding detectivity D^* were 6×10^{-13} W and 1.18×10^{12} cm Hz^{0.5}/W, respectively.

1 Introduction

In recent years, a lot of research has been focused on semiconductor-based ultraviolet (UV) photodiodes. Photodiodes operating in the short-wavelength UV region are vitally important for various commercial and military applications. Specifically, visible–blind UV photodiodes are being used in space communications, ozone layer monitoring and flame detection. Currently, light detection in the UV spectral range still relies on Si-based optical photodiodes. Even though these devices are quite sensitive to visible and infrared radiations, nevertheless, the responsivity in the UV region is considered relatively low because of the fact that the room temperature bandgap energy of Si is only 1.2 eV. With the optoelectronic devices start being fabricated on direct wide bandgap materials, being able to fabricate high-performance solid-state photodiodes which are sensitive to the UV regime has become a reality. For instance, GaN-based UV photodiodes have already become commercially available [1–6]. ZnSe-based UV photodiodes have also been successfully demonstrated [7].

For photodetector applications, the operation speed is always an important issue that requires a serious consideration. Previously, it has been shown that the electron mobility in AlGaIn/GaN heterostructures is limited by charged

dislocation and interface scatterings, and also the phase-separation effects [8]. These factors potentially may impose a restriction on the operation speed of GaN-based photodetectors. Alternatively, ZnO is another direct wide bandgap material that is also sensitive to the UV regime [9, 10]. A large exciton binding energy of 60 meV and wide bandgap energy of 3.37 eV at room temperature make ZnO a promising photonic material for applications in light-emitting diodes, laser diodes and UV photodiodes [11–13]. In fact, ZnO has attracted a substantial amount of attentions in recent years. High-quality ZnO epitaxial layers can be grown by metalorganic chemical vapour deposition [9], molecular beam epitaxy (MBE) [14], and pulsed laser deposition [15] on top of various substrates such as ZnO [10], sapphire [16] and epitaxial GaN layer [17]. Recently, it has been shown that it is possible to achieve ZnO epitaxial layers with high electron mobility using multi-step pulsed laser deposition (PLD) [7]. It has been reported that saturation velocity of ZnO is higher than that of GaN [18]. Compared with GaN, it has also been found that ZnO is less susceptible to irradiation effects [18]. Thus, ZnO-based photodetectors are potentially useful for high-speed UV light sensing. ZnO Schottky diodes and metal–semiconductor–metal photodiodes operating in the UV region have also been demonstrated [12]. Metal–semiconductor–metal (MSM) photodiodes with interdigitated Schottky contacts are deposited on top of an active layer. To achieve high-performance MSM UV photodiodes, a large Schottky barrier height is critically needed at metal–semiconductor interface. A large barrier height would lead to a small leakage current and high breakdown voltage which helped to improve the responsivity and photocurrent to dark current contrast ratio. To achieve a large Schottky barrier height on ZnO, metals with high work functions [19] are required. However, many of the high work function metals are not stable at high temperatures. In other words, severe inter-diffusion might occur at metal–ZnO interface. Iridium (Ir) is an interesting metal that has been used as stable Schottky contact of wide bandgap GaN [20–22]. Ir is a good conductor with superior thermal and chemical stabilities. GaN-based UV MSM photodetectors with IrO₂ and Schottky diodes with oxidised Ir/Ni Schottky contacts

© The Institution of Engineering and Technology 2007

doi:10.1049/iet-opt:20060084

Paper first received 11th September and in revised form 2nd December 2006

S.J. Young, S.J. Chang, Y.P. Chen and S.H. Liang are with the Institute of Microelectronics & Department of Electrical Engineering, National Cheng Kung University, Tainan 70101, Taiwan, Republic of China

L.W. Ji is with the Institute of Electro-Optical and Materials Science, National Formosa University, Yunlin 632, Taiwan, Republic of China

K.T. Lam is with the Institute of Applied Information, Leader University, Tainan 701, Taiwan, Republic of China

X.L. Du and Q.K. Xue are with the Institute of Physics, Chinese Academy of Sciences, Beijing 100080, People's Republic of China

Y.S. Sun is with the Department of Materials Science and Engineering, College of Machinery and Electronic Engineering, China University of Petroleum, Dongying City, Shandong 257061, People's Republic of China

E-mail: changsj@mail.ncku.edu.tw

have also been demonstrated [20–22]. However, neither the properties of Ir contacts on ZnO epitaxial layers nor the properties of ZnO-based devices with Ir contacts could be found in the literature to our knowledge. In this work, we report the growth of ZnO epitaxial layers by MBE and the fabrication of ZnO-based MSM photodetectors with Ir electrodes. Noise behaviours of the fabricated photodetectors will also be discussed.

2 Experiments

Samples used in this study were grown by radio frequency (rf) plasma-assisted MBE (Omni Vac) on sapphire (0001) substrates. The base pressure in the growth chamber was $\sim 1 \times 10^{-10}$ Torr. The source material of Zn was elemental Zn (6 N) evaporated from a commercial Knudsen cell (Crea Tech). Active oxygen and nitrogen radicals were separately produced by two rf-plasma systems (SVTA). The flow rate of oxygen/nitrogen gas was controlled by a mass flow controller (ROD-4, Aera). After degreased in trichloroethylene and acetone, sapphire substrates were etched in $\text{H}_2\text{SO}_4:\text{H}_3\text{PO}_4 = 3:1$ at 110°C for 30 min followed by rinsing in deionised water. The sapphire substrates were then loaded into the growth chamber. We then exposed the sapphire substrates to oxygen radicals for 30 min at 180°C with 350 W rf power and 2.5 sccm oxygen flux so as to form oxygen-terminated sapphire surface [23]. It should be noted that oxygen termination will result in anion-polar film, whereas aluminum termination, the cation polarity. We subsequently performed nitridation at 180°C for 1 h with 480 W rf power and 3.0 sccm nitrogen flux. After nitridation, a very thin AlN layer (~ 2 nm) will be formed with a 30° in-plane rotation of its lattice with respect to that of sapphire substrates. After nitridation, we grew a 1000 nm thick unintentionally doped ZnO epitaxial layer with conventional two-step growth method, i.e. a low-temperature buffer layer growth at 400°C and a high-temperature growth at 650°C . We subsequently annealed the ZnO epitaxial layer insituly at 750°C . At this moment, we observed 3×3 reconstruction pattern which indicates O-polar of our ZnO films [24]. From Hall measurement, it was found that carrier concentration and resistivity of the as-grown ZnO films at room temperature were 1.71×10^{16} per cm^3 and $13.8 \Omega \text{ cm}$, respectively. The samples were then characterised by photoluminescence (PL) and X-ray diffraction (XRD).

ZnO MSM photodetectors were then fabricated. Prior to the deposition of contact electrodes, wafers were dipped in acetone and methanol to clean the surface. We then used mesa etching for device isolation. An Ir film of 100 nm thickness was subsequently deposited onto the sample surface by e-gun evaporation to serve as metal contacts. Standard lithography and lift-off were then performed to realise the interdigitated contact pattern. The fingers of the Ir contact electrodes were $13 \mu\text{m}$ wide and $146 \mu\text{m}$ long with $8 \mu\text{m}$ spacing. The active area of the whole device was $146 \times 146 \mu\text{m}^2$. In some cases, we subsequently annealed the fabricated photodetectors at 500°C . Photocurrent and dark current of the fabricated photodetectors were then measured by an HP4145B semiconductor parameter analyser. Spectral responsivity measurements were also performed using a light source (Oriental Optical System) which employed a 250 W xenon arc lamp and a monochromator covering the range of 300–600 nm. Low-frequency noises of the fabricated photodetectors were also measured in the frequency range of 1 Hz–100 kHz using a low noise current preamplifier and an HP35670A fast Fourier transform spectrum analyser.

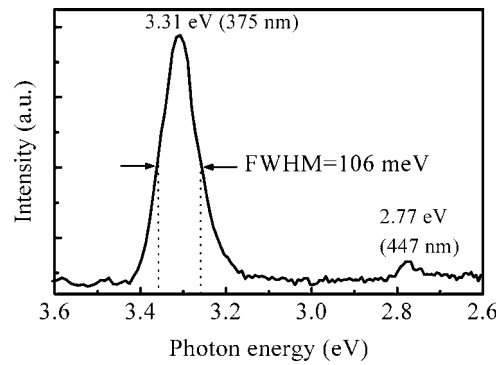


Fig. 1 Room temperature PL spectrum of epitaxial ZnO films

3 Results and discussion

Fig. 1 shows room temperature PL spectrum of our ZnO epitaxial films. It was found that we observed a strong excitonic related PL peak at 3.31 eV (375 nm) and a very weak green band emission at 2.77 eV (447 nm). It was also found that full width half maximum (FWHM) of the excitonic related PL peak was only 106 meV [16]. Furthermore, it was found that the intensity ratio between excitonic band and green band emission was extremely large and no deep-level broadband luminescence was observed. These results all indicate good crystal quality of our ZnO epitaxial layers [8]. Fig. 2 shows measured XRD spectrum of the 1000 nm thick ZnO epitaxial film prepared on sapphire substrate. The peak occurred at $2\theta = 41.9^\circ$ in the spectrum was originated from the (006) plane of sapphire substrate. We also observed a ZnO (002) XRD peak at $2\theta = 34.3^\circ$ with a FWHM of 0.18° . Such a result indicates that the ZnO film was preferentially grown in c-axis direction. The small FWHM of the ZnO (002) XRD peak again indicates good crystal quality of our samples.

Fig. 3 shows current–voltage (I – V) characteristics of the fabricated ZnO MSM photodetectors measured in dark and under illumination. During photocurrent measurements, the incident light wavelength was 370 nm, while the optical excitation intensity was kept at $10 \text{ mW}/\text{cm}^2$. Using thermionic emission theory and the dark currents measured in Fig. 3, we found that Schottky barrier heights at the non-annealed and 500°C -annealed Ir/ZnO interfaces were around 0.65 and 0.78 eV, respectively. In other words, dark current became smaller whereas photocurrent became larger after annealing. The smaller dark current and larger Schottky barrier height observed from the 500°C -annealed photodetector is probably because of the formation of IrO_2 after annealing. It is known that IrO_2 is

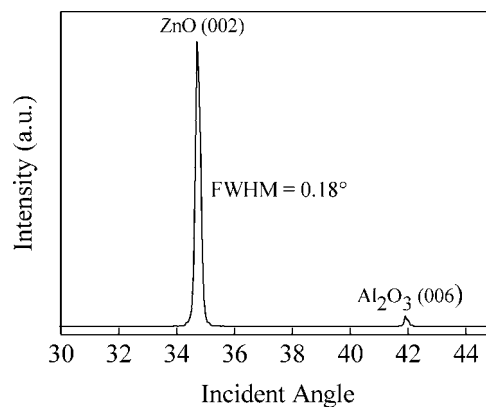


Fig. 2 XRD spectrum of the epitaxial ZnO films prepared on sapphire substrate

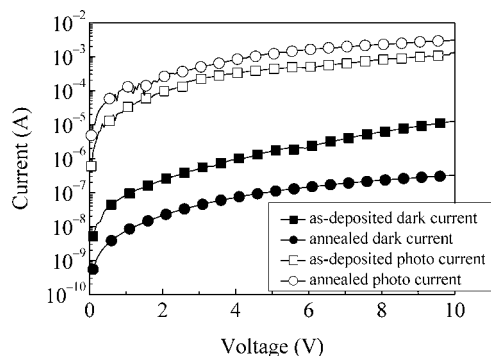


Fig. 3 I - V characteristics of the non-annealed and 500°C-annealed Ir/ZnO/Ir MSM photodetectors measured in dark (dark current) and under 370 nm illumination (photocurrent)

electrically conductive with high work function (>5.0 eV). It has been reported that IrO₂ forms good ohmic contacts on p-GaN [21] and forms good Schottky contacts on n-GaN [20]. We believe IrO₂ should also form good Schottky contacts on our n-ZnO epitaxial layers so that we should be able to effectively suppress the dark current. On the other hand, the increased photocurrent should also be attributed to the formation of IrO₂ after annealing. Since IrO₂ is highly transparent, more photons should be absorbed by the underneath ZnO.

Fig. 4 shows measured spectral responsivities of the Ir/ZnO/Ir MSM photodetectors. As shown in Fig. 4, it was found that the photodetector responsivities were nearly constants in the below bandgap UV region (300–370 nm) while sharp cutoffs with a drop of two orders of magnitude occurred at approximately 370 nm. With an incident wavelength of 370 nm and 1 V applied bias, it was found that the maximum responsivities for the Ir/ZnO/Ir MSM photodetectors with and without thermal annealing were 0.18 and 0.13 A/W, respectively.

Fig. 5 shows transient response in current of the non-annealed ZnO MSM photodetectors. As we turned-off the UV lamp, it was found that photocurrent decayed rapidly and could be well described by the stretched-exponential function as often reported for persistent photocurrent I_{ppc} in crystalline semiconductor.

$$I_{ppc}(t) = I_0(t) \exp\left[-\left(\frac{t_x}{\tau}\right)^\beta\right] \quad (1)$$

where $I_0(t)$ is the current when the light excitation is removed, τ is the decay time constant and β is the decay exponent. Using exponential fit to these experimental data, we achieved a time constant of $\tau \sim 22$ ms. Previously, it has been reported that persistent

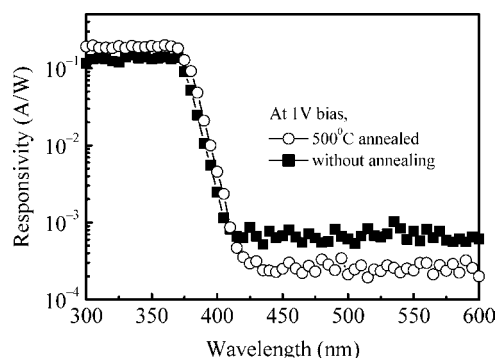


Fig. 4 Measured spectral responsivities of the annealed and non-annealed Ir/ZnO/Ir MSM photodetectors

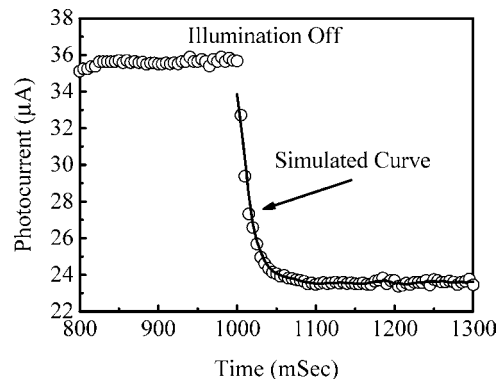


Fig. 5 Transient response in current of the non-annealed ZnO MSM photodiodes when the excitation source was removed

photoconductivity effect is commonly observed in ZnSe- and GaN-based photodetectors [25–29]. It has been shown that persistent photocurrent decay can be extremely long for GaN-based photodetectors [29]. The $\tau \sim 22$ ms decay time constant observed in this study seems to suggest that response speed of ZnO MSM UV photodetectors is faster than those of ZnSe- and GaN-based photodetectors with similar structures [25–27].

Fig. 6 shows low frequency noise spectra of the non-annealed ZnO MSM photodetectors with Ir electrodes. From these curves, it was found that measured noise power densities, $S_n(f)$, could be fitted well by $1/f^\gamma$ with $\gamma = 1$. The observed pure $1/f$ noise indicates that trapping states are distributed uniformly in energy for the device. For a given bandwidth of B , we could estimate the total square noise current by integrating $S_n(f)$ over the frequency range.

$$\begin{aligned} \langle i_n \rangle^2 &= \int_0^B S_n(f) df = \int_0^1 S_n(1) df \\ &+ \int_0^B S_n(f) df = S_0 [\ln(B) + 1] \end{aligned} \quad (2)$$

Here, we assumed $S_n(f) = S_n(1 \text{ Hz})$ for $f < 1$ Hz. Thus, the noise equivalent power (NEP) can be given by

$$\text{NEP} = \frac{\sqrt{\langle i_n \rangle^2}}{R} \quad (3)$$

where R is the responsivity of the photodetectors. The normalised detectivity, D^* , could then be determined by

$$D^* = \frac{\sqrt{A} \sqrt{B}}{\text{NEP}} \quad (4)$$

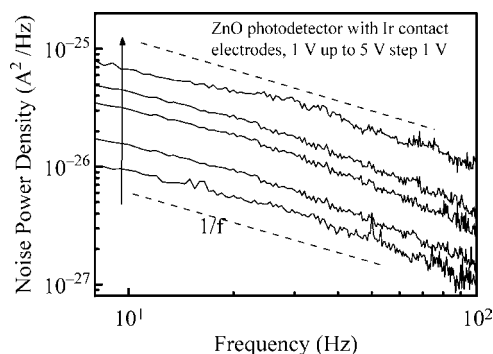


Fig. 6 Low-frequency noise spectra of the Ir/ZnO/Ir MSM photodetectors

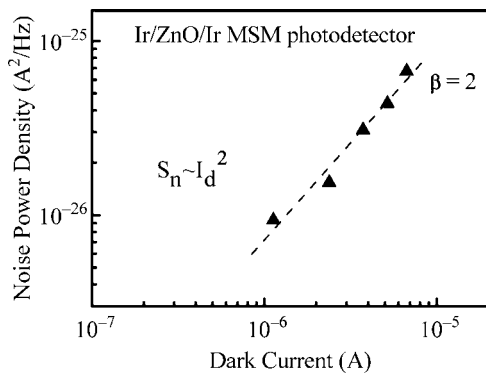


Fig. 7 Noise power densities measured at 10 Hz as a function of current for the Ir/ZnO/Ir MSM photodetectors

where A and B are the area of the photodetector and the bandwidth, respectively. For a given bandwidth of 100 Hz and a 1 V applied bias, we found that NEP and corresponding detectivity D^* of our Ir/ZnO/Ir MSM photodetectors were 6×10^{-13} W and 1.18×10^{12} cm Hz^{0.5}/W, respectively. The large detectivity D^* observed in this study seems to suggest that Ir/ZnO/Ir MSM photodetectors perform better than ZnSe- and GaN-based MSM photodetectors [27, 30]. Fig. 7 shows noise power density as a function of current for the Ir/ZnO/Ir MSM photodetectors measured at 10 Hz. It was found that measured noise power densities could be fitted well by the following equation.

$$S_n(f) = K \left(\frac{I_d^\beta}{f^\gamma} \right) \quad (5)$$

where $S_n(f)$ is the spectral density of the noise power, K is a constant, I_d is the dark current, β and γ are two fitting parameters. From Fig. 7, it was found that β and γ were 2 and 1, respectively. Such a result agrees well with Kleinpenning's model that spectral density of $1/f$ noise should be proportional to I_d^2 [31]. In other words, $1/f$ noise induced increase in current is related to the modulation of Schottky barrier height by uniformly distributed trapping states in our photodetectors. It should be noted that we fabricated five non-annealed photodetectors and five 500°C-annealed photodetectors. It was found that the five non-annealed photodetectors all exhibit similar characteristics. The standard deviations of the measured results were all within 15%. The same standard deviations were also found for the five 500°C-annealed photodetectors.

4 Summary

In summary, ZnO epitaxial films were grown on sapphire substrates by MBE. Ir/ZnO/Ir MSM UV photodetectors were also fabricated. With an incident wavelength of 370 nm and 1 V applied bias, it was found that the maximum responsivities for the Ir/ZnO/Ir MSM photodetectors with and without thermal annealing were 0.18 and 0.13 A/W, respectively. Furthermore, it was found that NEP and corresponding detectivity D^* of the Ir/ZnO/Ir MSM photodetectors were 6×10^{-13} W and 1.18×10^{12} cm Hz^{0.5}/W, respectively.

5 Acknowledgments

This work was supported by the National Science Council under contract number NSC 95-2221-E-150-077-MY3.

6 References

- Chiou, Y.Z., Chang, S.J., Su, Y.K., Wang, C.K., Lin, T.K., and Huang, B.R.: 'Photo-CVD SiO₂ layers on AlGaIn and AlGaIn-GaN MOSFET', *IEEE Trans. Electron Dev.*, 2003, **50**, pp. 1748–1752
- Monroy, E., Muñoz, E., Sánchez, F.J., Calley, F., Calleja, E., Beaumont, B., Gibart, P., Muñoz, J.A., and Cussó, F.: 'High-performance GaN p-n junction photodetectors for solar ultraviolet applications', *Semicond. Sci. Technol.*, 1998, **13**, pp. 1042–1046
- Xu, G.Y., Salvador, A., Kim, W., Fan, Z., Lu, C., Tang, H., Morkoç, H., Smith, G., Estes, M., Goldenberg, B., Yang, W., and Krishnankutty, S.: 'High speed, low noise ultraviolet photodetectors based on GaN p-i-n and AlGaIn(p)-GaIn(i)-GaIn(n) structures', *Appl. Phys. Lett.*, 1997, **71**, pp. 2154–2156
- Biyikli, N., Kimukin, I., Aytur, O., and Ozbay, E.: 'Solar-blind AlGaIn-based p-i-n photodiodes with low dark current and high detectivity', *IEEE Photon. Technol. Lett.*, 2004, **16**, pp. 1718–1720
- Katz, O., Garber, V., Meyler, B., Bahir, G., and Salzman, J.: 'Anisotropy in detectivity of GaN Schottky ultraviolet detectors: Comparing lateral and vertical geometry', *Appl. Phys. Lett.*, 2002, **80**, pp. 347–349
- Palacios, T., Monroy, E., Calle, F., and Omnes, F.: 'High-responsivity submicron metal-semiconductor-metal ultraviolet detectors', *Appl. Phys. Lett.*, 2002, **81**, pp. 1902–1904
- Lin, T.K., Chang, S.J., Su, Y.K., Chiou, Y.Z., Wang, C.K., Chang, C.M., and Huang, B.R.: 'ZnSe homoepitaxial MSM photodetectors with transparent ITO contact electrodes', *IEEE Tran. Electron Dev.*, 2005, **52**, pp. 121–123
- Manfra, M.J., Pfeiffer, L.N., West, K.W., Stormer, H.L., Baldwin, K.W., Hsu, J.W.P., Lang, D.V., and Molnar, R.J.: 'High-mobility AlGaIn/GaN heterostructures grown by molecular-beam epitaxy on GaN templates prepared by hydride vapor phase epitaxy', *Appl. Phys. Lett.*, 2000, **77**, pp. 2888–2890
- Barnes, T.M., Leaf, J., Hand, S., Fry, C., and Wolden, C.A.: 'A comparison of plasma-activated N₂/O₂ and N₂O/O₂ mixtures for use in ZnO:N synthesis by chemical vapor deposition', *J. Appl. Phys.*, 2004, **96**, pp. 7036–7044
- Kato, H., Sano, M., Miyanoto, K., and Yao, T.: 'Homoepitaxial growth of high-quality Zn-polar ZnO films by plasma-assisted molecular beam epitaxy', *Jpn. J. Appl. Phys.*, 2003, **42**, L1002–L1005
- Alivov, Y.I., Kalinina, E.V., Cherenkov, A.E., Look, D.C., Ataev, B.M., Omaev, A.K., Chukichev, M.V., and Bagnall, D.M.: 'Fabrication and characterization of n-ZnO/p-AlGaIn heterojunction light-emitting diodes on 6H-SiC substrates', *Appl. Phys. Lett.*, 2003, **83**, pp. 4719–4721
- Liang, S., Sheng, H., Liu, Y., Huo, Z., Lu, Y., and Shen, H.: 'ZnO Schottky ultraviolet photodetectors', *J. Crystal Growth*, 2001, **225**, pp. 110–113
- Mang, A., Reimann, K., and Rübenacke, St.: 'Band gaps, crystal-field splitting, spin-orbit coupling, and exciton binding energies in ZnO under hydrostatic pressure', *Solid State Commun.*, 1995, **94**, pp. 251–254
- Setiawan, A., Vashaei, Z., Cho, M.W., Yao, T., Kato, H., Sano, M., Miyamoto, K., Yonenaga, I., and Ko, H.J.: 'Characteristics of dislocations in ZnO layers grown by plasma-assisted molecular beam epitaxy under different Zn/O flux ratios', *J. Appl. Phys.*, 2004, **96**, pp. 3763–3768
- Kaidashev, E.M., Lorenz, M., von Wenckstern, H., Rahm, A., Semmelhack, H.C., Han, K.H., Benndorf, G., Bundesmann, C., Hochmuth, H., and Grundmann, M.: 'High electron mobility of epitaxial ZnO thin films on c-plane sapphire grown by multistep pulsed-laser deposition', *Appl. Phys. Lett.*, 2003, **82**, pp. 3901–3903
- Sakurai, K., Iwata, D., Fujita, S., and Fujita, S.: 'Growth of ZnO by molecular beam epitaxy using NO₂ as oxygen source', *Jpn. J. Appl. Phys.*, 1999, **38**, pp. 2606–2608
- Ko, H.J., Chen, Y.F., Hong, S.K., and Yao, T.: 'MBE growth of high-quality ZnO films on epi-GaN', *J. Crystal Growth*, 2000, **209**, pp. 816–821
- Pintilie, L., and Pintilie, I.: 'Ferroelectrics: New wide-gap materials for UV detection', *Mater. Sci. Eng. B*, 2001, **80**, pp. 388–391
- Auret, F.D., Goodman, S.A., Hayes, M., Legodi, M.J., van Laarhoven, H.A., and Look, D.C.: 'Electrical characterization of 1.8 MeV proton-bombarded ZnO', *Appl. Phys. Lett.*, 2001, **79**, pp. 3074–3076
- Kim, J.K., Jang, H.W., Jeon, C.M., and Lee, J.L.: 'GaN metal-semiconductor-metal ultraviolet photodetector with IrO₂ Schottky contact', *Appl. Phys. Lett.*, 2002, **81**, pp. 4655–4657
- Kim, J.K., and Lee, J.L.: 'GaN MSM ultraviolet photodetectors with transparent and thermally stable RuO₂ and IrO₂ Schottky contacts', *J. Electrochem. Soc.*, 2004, **151**, G190–G195

- 22 Jang, H.W., and Lee, J.L.: 'Transparent Ohmic contacts of oxidized Ru and Ir on p-type GaN', *J. Appl. Phys.*, 2003, **93**, pp. 5416–5421
- 23 Mei, Z.X., Wang, Y., Du, X.L., Ying, M.J., Zeng, Z.Q., Zheng, H., Jia, J.F., Xue, Q.K., and Zhang, Z.: 'Controlled growth of O-polar ZnO epitaxial film by oxygen radical preconditioning of sapphire substrate', *J. Appl. Phys.*, 2004, **96**, pp. 7108–7111
- 24 Chen, Y.F., Ko, H.J., Hong, S.K., and Yao, T.: 'Layer-by-layer growth of ZnO epilayer on Al₂O₃(0001) by using a MgO buffer layer', *Appl. Phys. Lett.*, 2000, **76**, pp. 559–561
- 25 Seghier, D., and Gislason, H.P.: 'Investigation of persistent photoconductivity in nitrogen-doped ZnSe/GaAs heterojunctions grown by MBE', *J. Crystal Growth*, 2000, **214**, pp. 511–515
- 26 Hu, G.J., Zhang, L., Dai, L.N., Chen, L.Y., and Tamargo, M.C.: 'Persistent photoconductivity in Ga delta-doped ZnSe', *Solid State Commun.*, 1999, **111**, pp. 631–634
- 27 Wang, C.K., Chang, S.J., Su, Y.K., Chiou, Y.Z., Chang, C.S., Lin, T.K., Liu, H.L., and Tang, J.J.: 'High detectivity GaN metal–semiconductor–metal UV photodetectors with transparent tungsten electrodes', *Semicond. Sci. Technol.*, 2005, **20**, pp. 485–489
- 28 Katz, O., Bahir, G., and Salzman, J.: 'Persistent photocurrent and surface trapping in GaN Schottky ultraviolet detectors', *Appl. Phys. Lett.*, 2004, **84**, pp. 4092–4094
- 29 Salis, M., Anedda, A., Quarati, F., Blue, A.J., and Cunningham, W.: 'Photocurrent in epitaxial GaN', *J. Appl. Phys.*, 2005, **97**, Art. No. 033709
- 30 Vigué, F., Tournié, E., and Faurie, J.P.: 'Evaluation of the potential of ZnSe and Zn(Mg)BeSe compounds for ultraviolet photodetection', *IEEE J. Quan. Electron.*, 2001, **37**, (No. 9), pp. 1146–1152
- 31 Kleinpenning, T.G.M.: 'Low-frequency noise in Schottky barrier diodes', *Solid-State Electron.*, 1979, **22**, pp. 121–128